IARJSET

ISSN (O) 2393-8021, ISSN (P) 2394-1588

International Advanced Research Journal in Science, Engineering and Technology

Vol. 8, Issue 11, November 2021

DOI: 10.17148/IARJSET.2021.81114

NUMERICAL SIMULATION OF SECONDARY INJECTION IN C-D NOZZLE IN THRUST

Kuppuraj.A[1] , Nagamanickam.N[2] , Praveen .T[3] , Yuvaraj .G[4]

[1]Assistant professor , Aeronautical engineering , Hindusthan college of engineering and technology , Coimbatore, Tamilnadu

[2,3,4]UG –Aeronatical Engineering ,Hindustan College of engineering and technology ,Coimbatore , Tamilnadu

Abstract: Fluidic thrust vectoring provides an additional control variable that offers many benefits in terms of maneuverability and control effectiveness in the new generation aircrafts and missiles. Thrust vectoring capabilities make the satisfaction of take-off and landing requirements easier. Fluidic thrust vectoring continues to work at low dynamic pressures, where other control technologies are less effective, making it a more valuable and dynamic in flight envelope. Additionally, thrust vectoring could increase conventional controls for some control power to trim the aircraft and thus reduce cruise trim drag. In this paper, an attempt has been made to numerically study the effect of thrust vectoring using shock vector method for various pressure ratios (Nozzle inlet pressure to Secondary injection Pressure) and the jet deflection angles are obtained. Also aims to study the effect of nozzle blockage effects for each pressure ratios. The numerical study includes two different inlet pressure conditions namely 9 and 12 bars, with the secondary injection pressure ratio varied from 9 to 15 bars. The numerical study is based on the K-epsilon turbulence model with enhanced wall treatment to capture the complex flow phenomena occurring on upstream and downstream of the secondary injection port. The primary jet decay characteristics at the nozzle exit and the side forces created on the nozzle walls are studied.

Key words: C-D nozzle, Thrust vectoring, Flow deflection, flow separation, fluidic thrust vectoring, shock vector.

INTRODUCTION

CONVERGING AND DIVERGING

The usual configuration for a converging diverging (C-D) nozzle is shown in the figure. Gas flows through the nozzle from a region of high pressure to one of low pressure. The chamber is usually big enough so that any flow velocities here are negligible. The pressure here is denoted by the symbol p_c. Gas flows from the chamber into the converging portion of the nozzle, past the throat, through the diverging portion and then exhausts into the ambient as a jet. The pressure of the ambient is referred to as the 'back pressure' and given the symbol p_b.

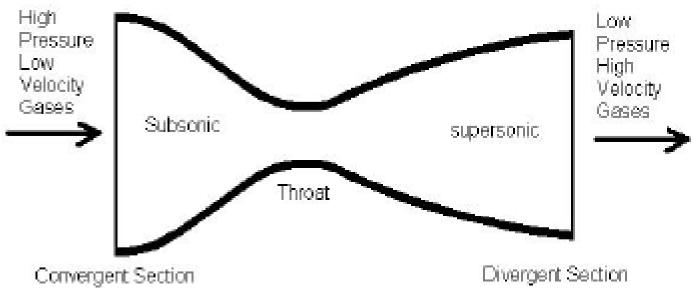

FIGURE:1 Converging and Diverging

A simple example

To get a basic feel for the behavior of the nozzle imagine performing the simple experiment shown in figure 2. Here we use a converging diverging nozzle to connect two air cylinders. Cylinder A contains air at high pressure, and takes the place of the chamber. The CD nozzle exhausts this air into cylinder B, which takes the place of the tank.

ISSN (O) 2393-8021, ISSN (P) 2394-1588
International Advanced Research Journal in Science, Engineering and Technology
Vol. 8, Issue 11, November 2021
DOI: 10.17148/IARJSET.2021.81114

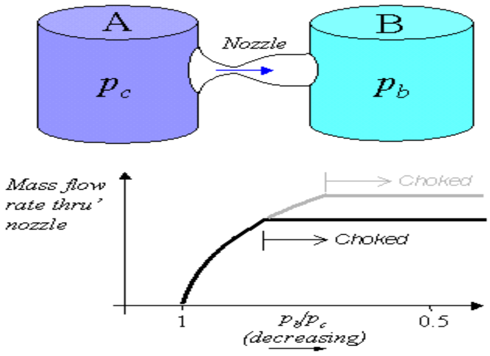

Figure 2. A simple experiment

Imagine you are controlling the pressure in cylinder B, and measuring the resulting mass flow rate through the nozzle. You may expect that the lower you make the pressure in B the more mass flow you'll get through the nozzle. This is true, but only up to a point. If you lower the back pressure enough you come to a place where the flow rate suddenly stops increasing all together and it doesn't matter how much lower you make the back pressure you can't get any more mass flow out of the nozzle. We say that the nozzle has become 'choked'. You could delay this behavior by making the nozzle throat bigger but eventually the same thing would happen. The nozzle will become choked even if you eliminated the throat altogether and just had a converging nozzle.

The reason for this behaviour has to do with the way the flows behave at Mach 1, i.e. when the flow speed reaches the speed of sound. In a steady internal flow the Mach number can only reach 1 at a minimum in the cross-sectional area. When the nozzle isn't choked, the flow through it is entirely subsonic and, if you lower the back pressure a little, the flow goes faster and the flow rate increases. As you lower the back pressure further the flow speed at the throat eventually reaches the speed of sound. Any further lowering of the back pressure can't accelerate the flow through the nozzle anymore, because that would entail moving the point where M=1 away from the throat where the area is a minimum, and so the flow gets stuck. The flow pattern downstream of the nozzle can still change if you lower the back pressure further, but the mass flow rate is now fixed because the flow in the throat is now fixed too.

The changes in the flow pattern after the nozzle has become choked are not very important in our thought experiment because they don't change the mass flow rate. They are, however, very important however if you were using this nozzle to accelerate the flow out of a jet engine or rocket and create propulsion, or if you just want to understand how high-speed flows work.

1.2 Numerical model

The base SERN model for this study is a slightly modified version of the model used by carbon and slyer. The three-dimensional view of this model. The schematic view of the model with detailed dimensions and injection positions. In the schematic diagram, Ht represents the height of the throat, Xramp is the position of ramp injection calculated from the starting point of the ramp. CD dotted line represents the exit plane of the SERN.

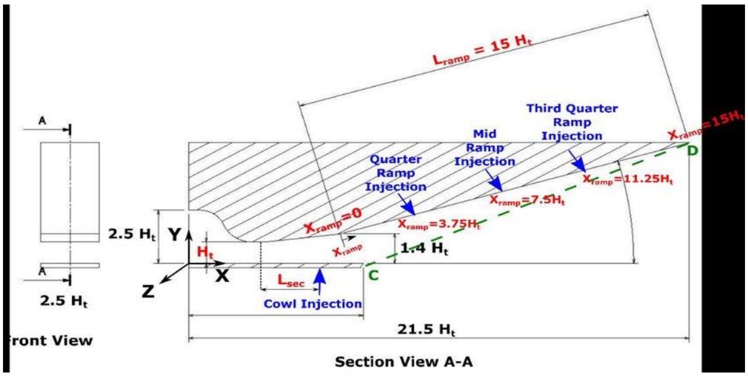

Figure 3:. SERN configuration with injection location b) schematic diagram with injection location.

Lsec indicates the location of the cowl injection from the throat . The SERN flow flows in the positive X direction. The width of the SERN in the Z direction is constant throughout the length of the SERN. A 3D domain model is constructed using ANSYS design modeler, and an unstructured mesh is generated using ANSYS meshing tool. ANSYS CFX solver is used to perform the computations. The inlet boundary is specified with total pressure; the opening

Vol. 8, Issue 11, November 2021

DOI: 10.17148/IARJSET.2021.81114

boundary is specified with static pressure. To reduce the computation time and cost XY plane is considered as symmetry boundary. The walls of SERN is specified as no-slip adiabatic walls.

As specified in the study of Lva and Xua RNG k-ε turbulence model is used. The reference pressure temperature is considered as 1 atm and 288 K, respectively. The residual target achieved in all the simulations is 10-6.

EXHAUST FLOW DEFLECTION

An alternative to nozzle manipulation is direct flow manipulation by use of post-nozzle exit vanes or paddles. Thrust vectoring by way of exhaust flow deflection was found on WWII era German V-2 rockets. The V-2 rockets used four graphite vanes mounted in the hot exhaust flow to steer the rocket toward its intended target. The deflection of the four vanes, were controlled by a series of gyroscopes. Berrier and Mason researched the effectiveness of a much more modern, paddle-based system in 1988. They examined the effects of many variables associated with the design and placement of the paddles including paddle curvature, paddle location relative to the nozzle, the number of paddles used and the degree of deflection. They tested several paddle configurations on a small-scale single engine simulation system which used compressed air as the source of its power. It was immediately noticed that spoon-shaped paddles deflected the flow to a greater degree than paddles that had curvature in the radial direction only. The researchers note, that for every case, increased flow deflection always resulted in increased thrust losses.

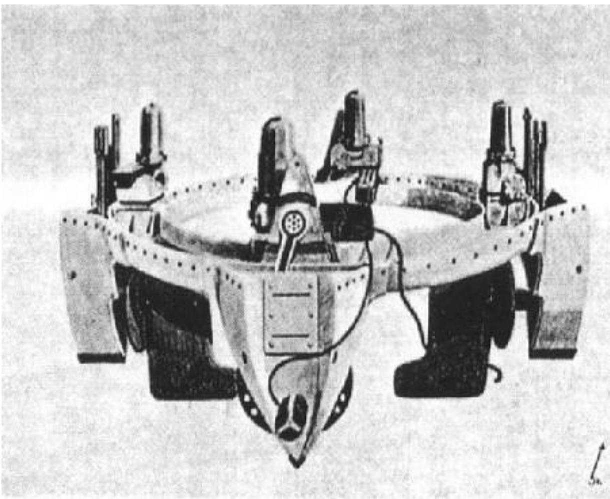

Figure 4: Graphite thrust vectoring vanes that were used on German V-2 rocket

SECONDARY FLUIDIC INJECTION

Thrust vectoring by means of secondary fluidic injection follows the same principle of nozzle manipulation, but it does not alter the physical configuration of the nozzle. By injecting a second fluid (air from the engine compressor or fan), the exhaust flow can be manipulated and controlled. The injected fluid serves to create variable artificial nozzle boundaries. Nozzles utilizing fluidic vectoring techniques can have better stealth characteristics and weigh less because they can be constructed as fixed geometry nozzles and are not required to have complex adjustable hardware. The three primary techniques of fluidic thrust vectoring that have been studied include counter flow, shock vector control and throat shifting. While the methods may vary, they can be compared to each other in terms of efficiency. Efficiency for these nozzles is given as the degree of vectoring achieved per percent of secondary flow required as compared to the primary nozzle flow.

EXPERIMENTAL APPROACH

Experimental study is conducted at the supersonic free jet facility of Advanced Propulsion and Laser Diagnostic Laboratory (APLD) in IIST, Thiruvananthapuram. The free jet facility consists of an TM ELGI (Model: E18-10) single-stage air cooled screw compressor, a TM GEM air-dryer, a reservoir tank with a pressure storage capacity of 12 bar as shown in Figure 1. The stagnation temperature is assumed to be 300K and all the pressures are absolute. Controlled flow of air inside the test section is done by PID controller. Pressure measurements are required at the wall surface of the expanding nozzle and this is done by unsteady transducers. TM Kulite (Model: XCQ-152 Series) transducers are used for the pressure measurements. The locations of transducers are shown in Fig. 2. Three nozzle configurations (2D) are manufactured, in which slots where cut in two of them to give angled injections of 15 and 30

DOI: 10.17148/IARJSET.2021.81114

with respect to the tangent of the nozzle contour. The nozzle is designed to produce an exit Mach number of 2, using the method of characteristics. The injector slot width is 1 mm. The detailed dimensions of the nozzle will be discussed in the next subsection. For each nozzle configurations, three sets of experiments are conducted for cross flow absolute pressures of 3 bar, 4 bar and 5 bar. For the injections cases, the pressures at the injector were 2 bar and 3 bar absolute. Unsteady pressure transducers are used to measure the pressure at different locations (Fig. 2). Additionally Schlieren images were taken with a Pixelfly camera (make PCO) with 1392×1040 resolution and 14 bit dynamic range.

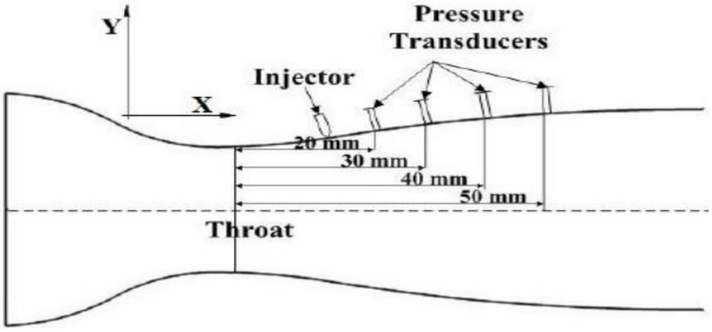

Figure:5 Layout of the experimental facility

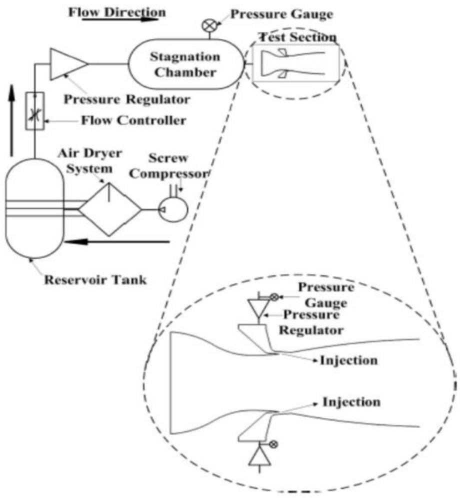

Figure: 6 Location of the pressure transducers

Experiments were conducted on different operating conditions. Table 5 shows the operating conditions adopted and terminology used for different configurations. For a nozzle with no injection, the number at the end in the terminology denotes the cross flow stagnation pressure. For example NoInj_3 means the cross flow stagnation pressure used is of 3 bar. For injection cases, the first number denotes the injection angle, the second number denotes the cross flow stagnation pressure and the third number denotes the injection pressure. For example 15_3CF_2Inj means the cross flow stagnation pressure is 3 bar, and injection is given at an angle of 15 and 2 bar.

IARJSET

ISSN (O) 2393-8021, ISSN (P) 2394-1588

International Advanced Research Journal in Science, Engineering and Technology

Vol. 8, Issue 11, November 2021

DOI: 10.17148/IARJSET.2021.81114

Table: 5 Operating conditions and Terminology

Nozzle Config.	Exp. Conditions		Terminology
	Cross Flow Stagnation Pressure (bar)	Injection Pressure (bar)	
No Injection	3	-	NoInj_3
	4	-	NoInj_4
	5	-	NoInj_5
15°	3	2	15_3CF_2Inj
	3	3	15_3CF_3Inj
	4	2	15_4CF_2Inj
	4	3	15_4CF_3Inj
	5	2	15_5CF_2Inj
	5	3	15_5CF_3Inj
30°	3	2	30_3CF_2Inj
	3	3	30_3CF_3Inj
	4	2	30_4CF_2Inj
	4	3	30_4CF_3Inj
	5	2	30_5CF_2Inj
	5	3	30_5CF_3Inj

1.6 Boundary conditions

A pressure inlet boundary was used for nozzle inlet, secondary inlet and nozzle outlet where: Inlet: Primary Stagnation Pressure, Pop = 100 Psig, Primary Stagnation Temperature, Top= 258.5K

Outlet: Primary Nozzle Exit Pressure, Pep = 101068Pa

Secondary inlet: - Secondary to primary stagnation pressure ratio Pos/Pop=0.6. -Secondary injectant temperature Tos=272.2K. - Secondary injection slot to primary throat area ratio As/A*=0.05 -Injection location with respect to the primary flow Mach number Mp=1.904.

LITERATURE REVIEW

G. Anugrah, P. Raja, M. Deepu† and R. Sadanandan In the primary design requirements for a high thrust delivering converging-diverging rocket nozzle working at zero ambient pressure is a large area ratio. Due to over expansion, a nozzle designed for a low pressure upper atmosphere is less efficient at sea level where the ambient pressure is comparatively high. There are several innovative ideas proposed to take in to account of this problem, like the dual-bell nozzles, nozzles with fixed and temporary inserts, nozzles with active or passive gas injection etc.

Goliath Shanmugaraj, J V Muruga Lal Jeyan, Vijay Kumar Singh The poor flight performance at the off-design operating condition. Especially while operating at an over-expanded condition due to the over expanded flow at the ramp surface, a nose-up pitching moment is generated. In this study, to reduce this, various secondary injections are used at various locations on either of the cowl surface or ramp surface.

H.R. Noaman , Tang Hai Bin and Elsayed Khalil The effects of speed on the physical behaviour in combustion cylinder process in a diesel engine fueled with diesel. A numerical study was performed using the CFD software fluent at different engine speeds. All input factors such as compression ratio, spray angle, injection timing and input mass flow rate have been unchanged, and var...

Farzad Forghany , Mohammad Taeibe-Rahni , Abdollah Asadollahi-Ghohieh The current research attempted to apply a numerical investigation for external freestream-flow influence on thrust-vector control. The freestream-flow Mach numbers varying from 0.05 to 1.1 were studied at different flow conditions. Computational modeling and simulation of a converging diverging nozzle with shock-vector control structure was achieved with utilizing the Unsteady-RANS approach and SpalartAllmaras turbulence model. The present investigation has shown that, freestream-flow is an essential parameter on performance of shock-vector nozzle. Numerical results demonstrate that, increasing freestream Mach number would reduce the thrust-vectoring effectiveness.

DOI: 10.17148/IARJSET.2021.81114

Jerin John, Subanesh Shyam. R., Aravind Kumar T. R., Naveen. N., Vignesh. R., Krishna Ganesh. B., Sanal Kumar V. R Numerical studies have been carried out using a validated two-dimensional RNG k-epsilon turbulence model for the design optimization of a thrust vector control system using shock induced supersonic secondary jet. Parametric analytical studies have been carried out with various secondary jets at different divergent locations, jet interaction angles, jet pressures.
R. Chouichaa, *, M. Sellamb , S. Bergheula The transverse injection of a fluid in a supersonic flow generates a complex flow involving asymmetric detachment due to an adverse pressure gradient, various interactions and reflections of shocks and vortex zones governing the mixture of flows downstream. Zones of high pressure upstream and low pressure downstream of the jet cause a natural inclination of the jet downstream of the flow.
C. Suresh1 G. Dinesh Kumar, D.Gowrishankar Fluidic thrust vectoring provides an additional control variable that offers many benefits in terms of maneuverability and control effectiveness in the new generation aircrafts and missiles. Thrust vectoring capabilities make the satisfaction of take-off and landing requirements easier. Fluidic thrust vectoring continues to work at low dynamic pressures, where other control technologies are less effective, making it a more valuable and dynamic in flight envelope. Additionally, thrust vectoring could increase conventional controls for some control power to trim the aircraft and thus reduce cruise trim drag .
Joel H. Marshall Utah State University A thrust augmented nozzle for hybrid rocket systems is investigated. The design lever-ages 3-D additive manufacturing to embed a helical fuel port into the thrust chamber of a hybrid rocket burning gaseous oxygen and ABS plastic as propellants. The helical port significantly increases how quickly the fuel burns, resulting in a fuel-rich exhaust exiting the nozzle.

METHODOLOGY

The Experimentation and Computer -aided engineering (CAE) are the important tools used for the analysis of the system. CFD is one of the CAE tools, designed for analyzing the problem involved in the fluid motion, heat exchange etc. It provides good approximate result and has certain advantage over the experiment approach. The optimization of models is easily done by the computer-based software like AUTOCAD, ANSYS Design modular and solid works.

ANSYS SOLVER

ANSYS is a world's leading widely distributed and popular commercial CAE package. It is widely used by designers/analysts in industries such as aerospace, automotive, manufacturing, nuclear, electronics, biomedical and more. This enables designers to simulate design performance directly on the desktop. In this way, it provides fast, efficient and cost effective product development from design concept. It offers engineering simulation solution sets in engineering solution that a design process requires. Companies in wide variety of industries use ANSYS Software. It uses CFD and FEM and various other programming algorithms for simulating and optimizing various design problems. ANSYS has many sub parts out of which I will use FLUENT.ANSYS Fluent uses CFD for analysis and is mainly used for simulation of fluid mechanics and thermodynamic problems. Data of various fluid and solid materials are already fed in to the ANSYS database which we use.

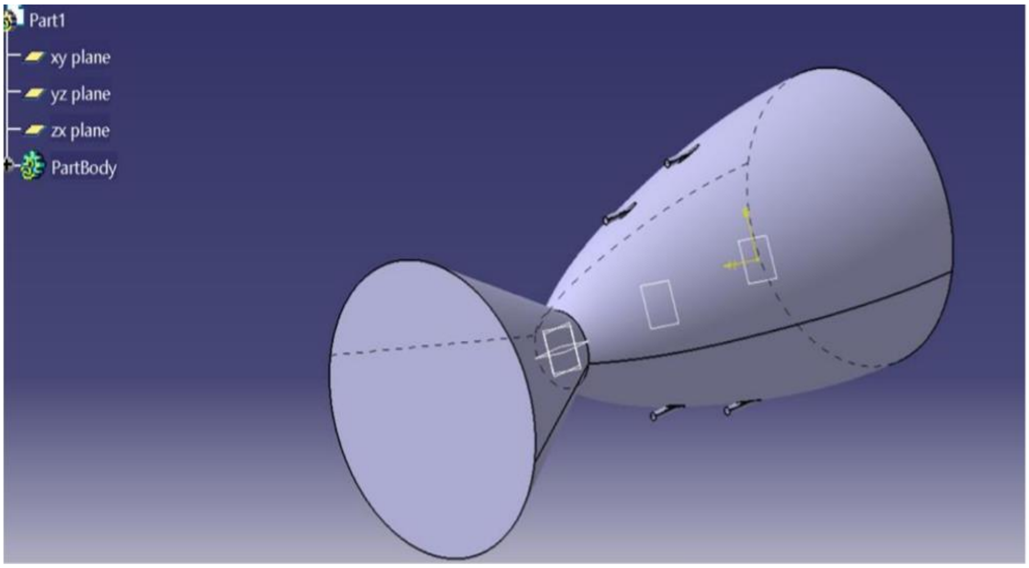

IARJSET
ISSN (O) 2393-8021, ISSN (P) 2394-1588
International Advanced Research Journal in Science, Engineering and Technology
Vol. 8, Issue 11, November 2021
DOI: 10.17148/IARJSET.2021.81114

Capture proximity	yes
Proximity min size	Default(1.6082 mm)
Bounding box Diagonal	3216.5 mm
Average Surface area	4.8145 +005 mm^2
Nodes	103963
Element	540154
Proximity size function sources	Faces and Edges
Boundary	Nozzle walls

TABLE :1 DETAILS OF MESH

BOUNDARY CONDITIONS

Pressure inlet	800kpa
Temperature inlet primary	500k
Temperature inlet secondary	1000k
Hot gas used	Hydrogen fluride
Operating Pressure	38 kpa
Pressure ratio	1.05(sonic at thrust)
outlet	Pressure outlet with zero static pressre
walls	Non slippery walls

GEOMETRY SPECIFICATION

Inlet diameter	1150 mm
Outlet diameter	1150 mm
Throat diameter	300 mm
Injector length	220 mm
Injector diameter	30 mm
Nozzle length	2775 mm

SOLVER SETUP:

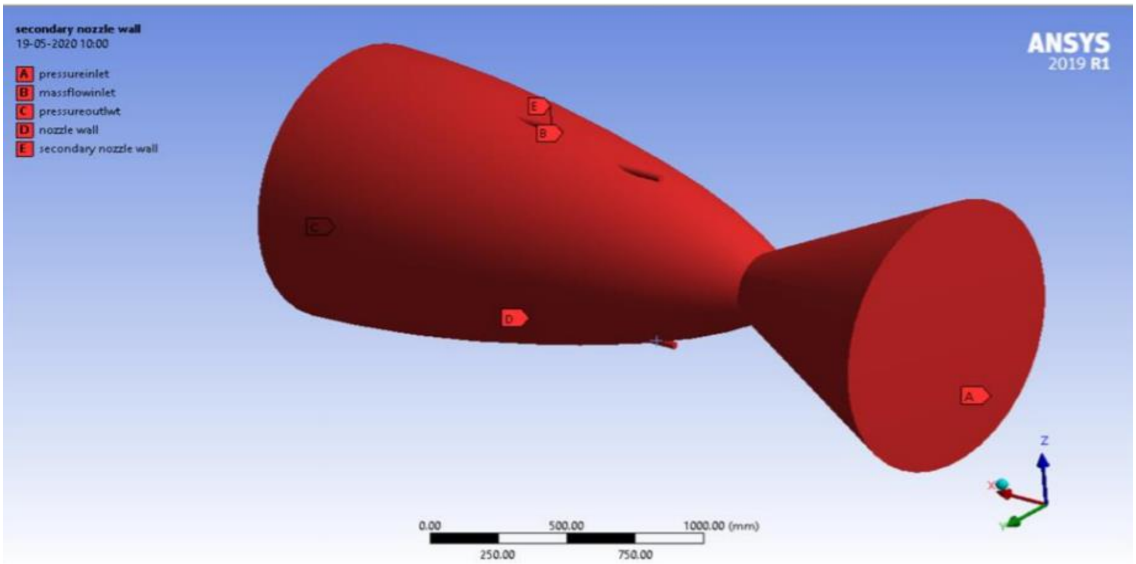

Assumptions made for this problem are follows,

- **K - ω Turbulence** – SST – Viscous Heating is selected to meticulous features of Fluid flow over the body
- Density based Solver is selected to capture the Density – Pressure – Temperature Interaction
- Second Order Discretization is used to steer the solution towards Supersonic Flow
- FMG Initialization Coding is hooked up to avoid divergence of Solution

IARJSET

ISSN (O) 2393-8021, ISSN (P) 2394-1588

International Advanced Research Journal in Science, Engineering and Technology

Vol. 8, Issue 11, November 2021

DOI: 10.17148/IARJSET.2021.81114

GRID INDEPENDENCE STUDY

Grids or nodes are the points at which the transport equations of fluid flow are solved. These transport equations represent the spatial and time variation of different flow variables such as pressure, velocities in X, Y, Z directions, temperature, and turbulence properties etc. The partial differential quotients approximated as differential quotient for first order approximation with forward difference scheme as follows.

According to Taylor expansion, which numerically approximates property is given by,

$$\frac{\partial f(x)}{\partial x} = \lim_{\nabla x \to 0} \left(\frac{f(x+\Delta x) - f(x)}{\nabla x}\right)$$

Which represents the distance between centroids of two successive elements, tends to go to zero 0 the accuracy of the numerical solution tends to move towards the exact solution and the error diminishes. Thus, CFD results are highly depends on mesh count. More over mesh shape, mesh quality such as skewnes s, aspect ratio are also plays essential role in increasing the accuracy of the result. On the other hand, increase in mesh count needs more CPU power and time to solve the equations. Ultimately, this increases the computational cost and effort. Therefore, it is very important for a CFD user to play between accuracy of the result and computational cost.

$$f(x+\nabla x) = f(x) + \frac{\partial f(x)}{\partial x}\frac{\Delta x}{1!} + \frac{\partial^2 f(x)}{\partial x^2}\frac{(\Delta x)^2}{2!} + \frac{\partial^3 f(x)}{\partial x^3}\frac{(\Delta x)^3}{3!} + \ldots\ldots\ldots\ldots$$

With a coarse mesh, the study is initiated and the trial is continued with finer meshes. With increase in mesh count, accuracy of the solution increases and there will be a point reached at which even if the mesh count is increased further there will not be considerable variation of CFD results. At this point CFD results become independent of the mesh count. Mesh at this point is taken for further studies.

RESULTS AND DISCUSSION

A parametric study on injection mass flow rate (changing secondary stagnation pressure) with the same injection location and injection angle is done as mass flow rate of the injectant varies directly with the injection total pressure.

The strength (shock angle) of the primary bow shock inside nozzle increases with the secondary mass flow rate (by increasing the secondary stagnation pressure) as shown in figure 12. The origination point of the primary bow shock moves further upstream of the injector as the secondary mass flow rate increases (by increasing the secondary stagnation pressure). Leads to extended higher pressure region upstream of the injector as shown in figure:12

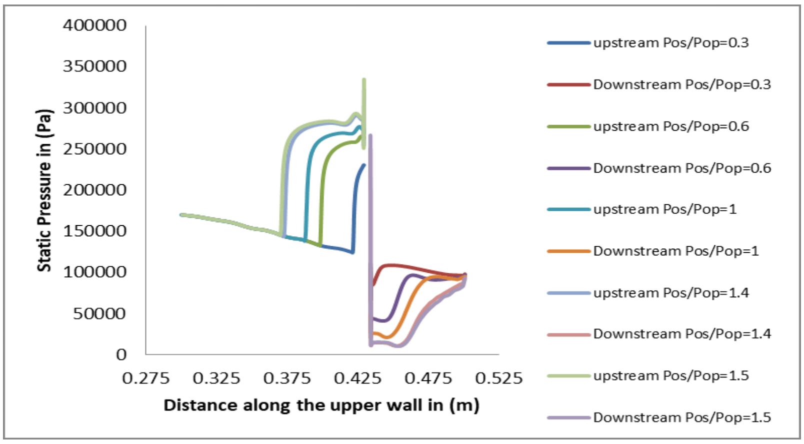

Figure:12 Effect of injection mass flow rate on injector wall static pressure

Discussion:

same as in primary bow shock, the strength of the separation increases as the secondary mass flow rate is increased (by increasing the secondary stagnation pressure). Stronger separation shock results into stronger injector upstream higher wall pressure region as shown in figure 12. Higher secondary mass flow rates (resulting from higher secondary stagnation pressure) also cause extended lower pressure regions downstream of the injector. As the injection mass flow

IARJSET

ISSN (O) 2393-8021, ISSN (P) 2394-1588

International Advanced Research Journal in Science, Engineering and Technology

Vol. 8, Issue 11, November 2021

DOI: 10.17148/IARJSET.2021.81114

rate is lowered, the reattachment point moves upstream on the primary nozzle wall in the aft section of the injector as shown in figure 13.

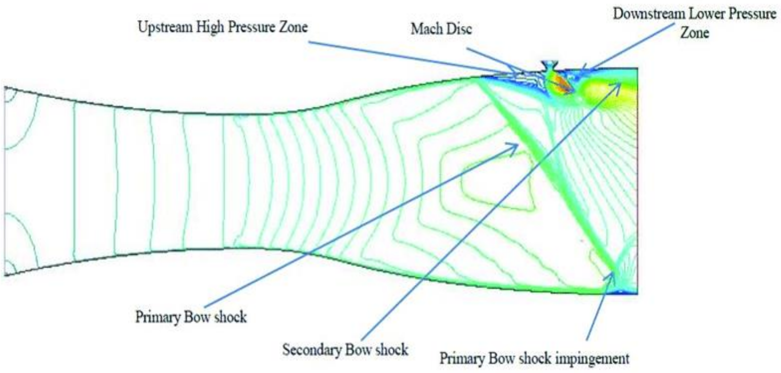

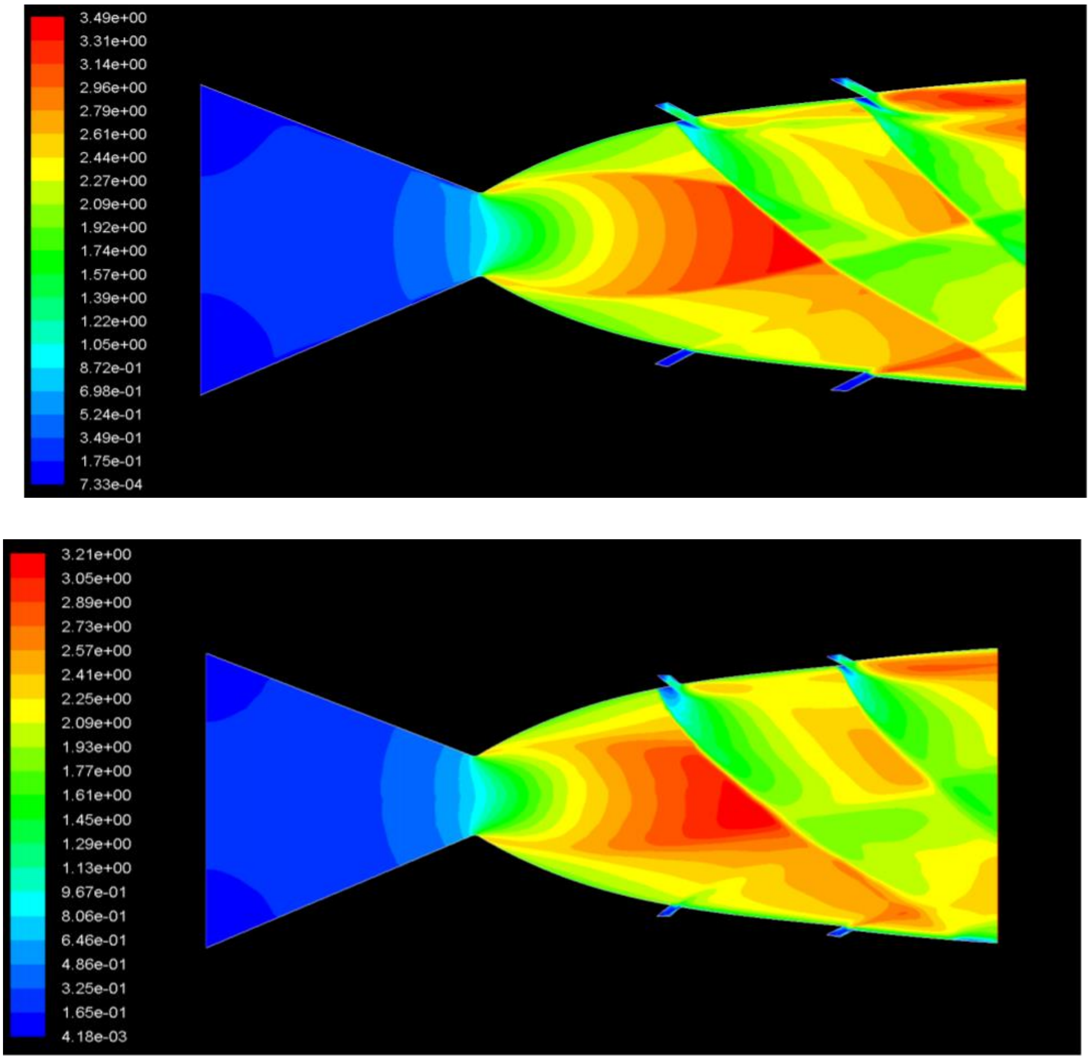

Figure 13 : Effect of injection mass flow rate on lower wall static pressure distribution .

In figure 13 the effect of increasing the inject ant mass flow rate on the lower wall it shows that no changes in the static pressure along the lower wall till reaching Pos/Pop=1.3 a very small shock impingement arises on the exit of the nozzle and when Pos/Pop increased to 1.4 and then 1.5 a significant shock impingement is shown leads to rise in the static pressure on the lower wall which effects the side force. The complex flow field with shock impingement setup by

International Advanced Research Journal in Science, Engineering and Technology
Vol. 8, Issue 11, November 2021
DOI: 10.17148/IARJSET.2021.81114

secondary injection inside primary supersonic flow was shown in Figure 14.

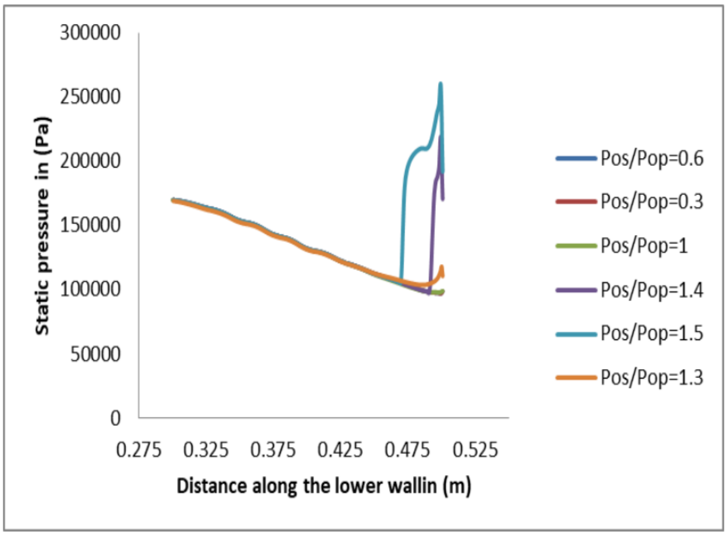

Figure 14: Flow field structure (Mach number contours) setup by secondary injection into primary nozzle flow.

CONCLUSION

A small scale two dimensional convergent divergent nozzle was used to investigate the performance of fluidic thrust vectoring using shock vector control method. A secondary injection port was formed by a slot normal to the diverging wall of the nozzle. The analysis was made for two different inlet pressure ratios of 9 and 12 bar. The velocities downstream of the nozzle are measured to find the flow deflections. It is observed that if the secondary injection pressure is increased above pressure ratio of 1, the flow separation dominates which leads to reverse flow inside the nozzle leading to divergence. A good agreement was observed for both the cases if the secondary injection pressure ratio is less than 1. The turning of the primary flow stream by the shock and the unbalanced pressure increase due to secondary flow injection, which is induced on the nozzle wall where the boundary layer upstream of the injection separates. Injection slot on the wall needs to be profiled out of the nozzle and not to impose new boundary condition on the nozzle wall itself which creates numerical artifacts and not physical solutions. This should be either just strait "pipe" section or convergent section exiting into the nozzle. the velocity contours mentioned the effects on the convergent and throat sections are taking its toll. Upper corners close to inlet are not properly resolved generating back flow region. Due to short curvature radius at throat, there is strange artifact on the velocity profile propagating downstream and mixing with compression waves that are typical for the convergent nozzle. The main supersonic flow reacts on the obstacle in the shape of secondary injection with the bow shock. This bow shock inflicts the adverse pressure gradient in the upstream zone of the injection, which consequently detaches the flow from the nozzle wall. In the separation zone there are 2 counter rotating vortices one can denote 2 vortices, primary longer close to incipient point and secondary counter rotating near the injection itself. Finally the two dimensional model is not very suitable for secondary injection thrust vectoring problems.

REFERENCES

1. R. Chouichaa, *, M. Sellamb , S. Bergheula a Laboratoire des Sciences Aéronautique, Institut D`Aéronautique et des Etudes Spatiales, Université Saad Dahlab-Blida1, BP 270, Route de Soumâa, Blida, Algeria b LMEE, Univ Evry, Université Paris-Saclay, 91020, Evry Cedex, France Received 10 September 2019; accepted 11 April 2020.
2. To cite this article: Gopinath Shanmugaraj et al 2020 J. Phys.: Conf. Ser. 1473 012002.
3. C. Suresh1 G. Dinesh Kumar, D.Gowrishankar 1 Assistant Professor, School of Aeronautical Sciences, Hindustan Institute of Technology & Science, Chennai, India.
4. R. Chouichaa, *, M. Sellamb , S. Bergheula a Laboratoire des Sciences Aéronautique, Institut D`Aéronautique et des Etudes Spatiales, Université Saad Dahlab-Blida1, BP 270, Route de Soumâa, Blida, Algeria b LMEE, Univ Evry, Université Paris-Saclay, 91020, , Evry Cedex, France Received 10 September 2019; accepted 11 April 2020.
5. Mohammad Azis khan, Y.N.V. Santhosh Kumar, M.Venkatesh Student, Assistant professor, Assistant professor Department of Aeronautical Engineering, Nimra Institute of Science and Technology, Vijayawada, India.
6. Jerin John, Subanesh Shyam. R., Aravind Kumar T. R., Naveen. N., Vignesh. R., Krishna Ganesh. B., Sanal Kumar V. R.
7. H.R. Noaman , Tang Hai Bin 1 and Elsayed Khalil 2 1 Beihang University, School of Astronautics, Beijing, China 2 Military Technical College, Aerospace Department, Cairo, Egypt.
8. Farzad Forghany a,⇑ , Mohammad Taeibe-Rahni b , Abdollah Asadollahi-Ghohieh c aDepartment of Mechanical and Aerospace Engineering,

Science and Research Branch, Islamic Azad University, Tehran, Iran bDepartment of Aerospace Engineering, Sharif University of Technology, Tehran, Iran c Civil Aviation Technology College, Tehran, Iran.
9. Prince raj .l, Rejith.P, Balu.R Noorul.islam center for higer education, kumaracoil, 629 180.
India Dean , Inter- Disciplnary studies,Noorul .Islam centre for higher education , Maracsibo,629 180 .India.
10. G. Anugrah, P. Raja, M. Deepu† and R. Sadanandan Department of Aerospace Engineering; Indian Institute of Space Science Technology, Thiruvananthapuram, Kerala-695547, India †Corresponding Author Email: deepu@iist.ac.in (Received November 12, 2018; accepted January 11, 2019).
11. Joel H. Marshall Utah State University Marshall, Joel H., "Thrust Augmented Nozzle for a Hybrid Rocket with a Helical Fuel Port" (2018). All Graduate Theses and Dissertations. 6915.
12. D.Swain1· S.K. Biswal2· B.P. Thomas1· S.S. Babu2· J. Philip1Received: 12 February 2018 / Accepted: 20 August 2018 / Published online: 25 October 2018© The Society for Experimental Mechanics, Inc.